

# Supplementary Material for CDS

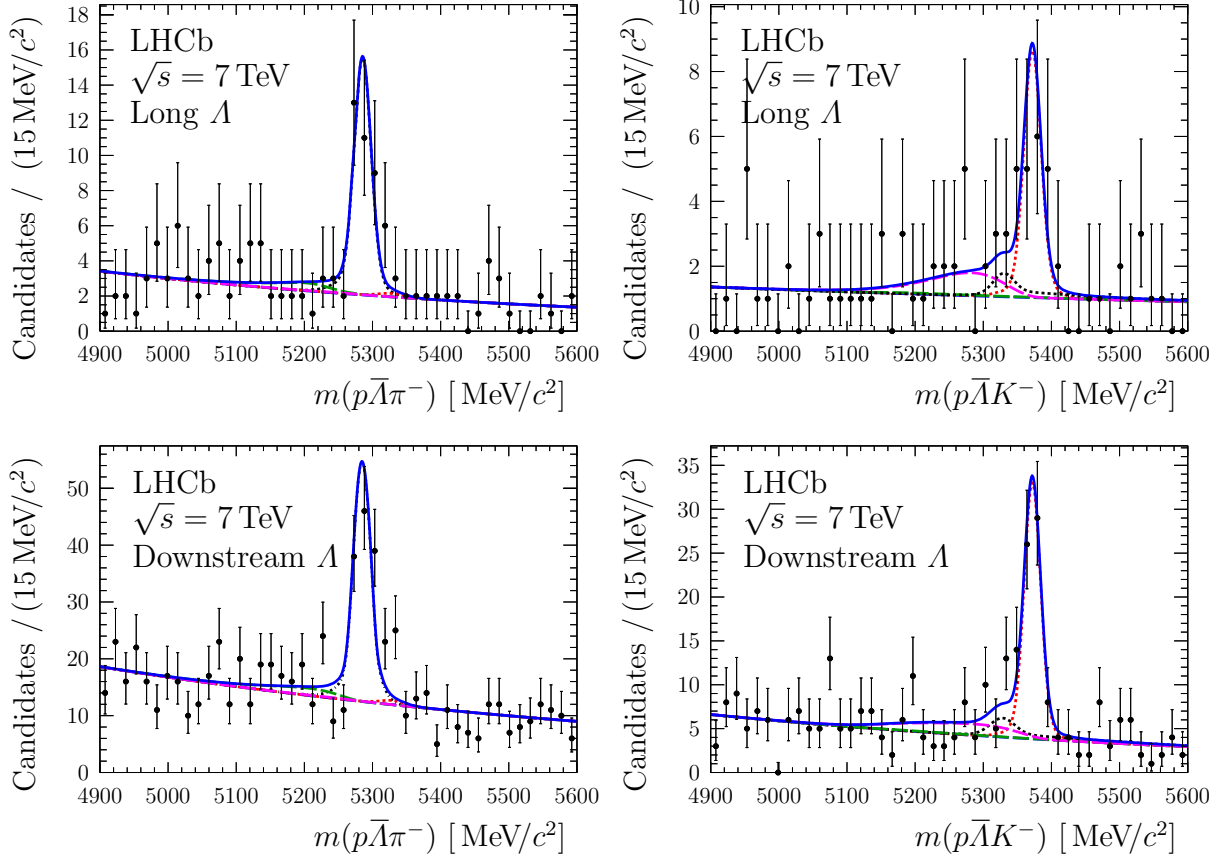


Figure 1: Mass distributions for  $b$ -hadron candidates for (left) the  $p\bar{\Lambda}\pi^-$  and (right) the  $p\bar{\Lambda}K^-$  sample for (top) the long and (bottom) the downstream 2011 categories. The black points represent the data, the solid blue curve the result of the fit, the black (red) dotted curve the  $B^0 \rightarrow p\bar{\Lambda}\pi^-$  ( $B_s^0 \rightarrow p\bar{\Lambda}K^-$ ) contribution, and the green (magenta) dashed curve the contribution from  $B^0 \rightarrow p\bar{\Sigma}^0\pi^-$  ( $B_s^0 \rightarrow p\bar{\Sigma}^0K^-$ ) decays.

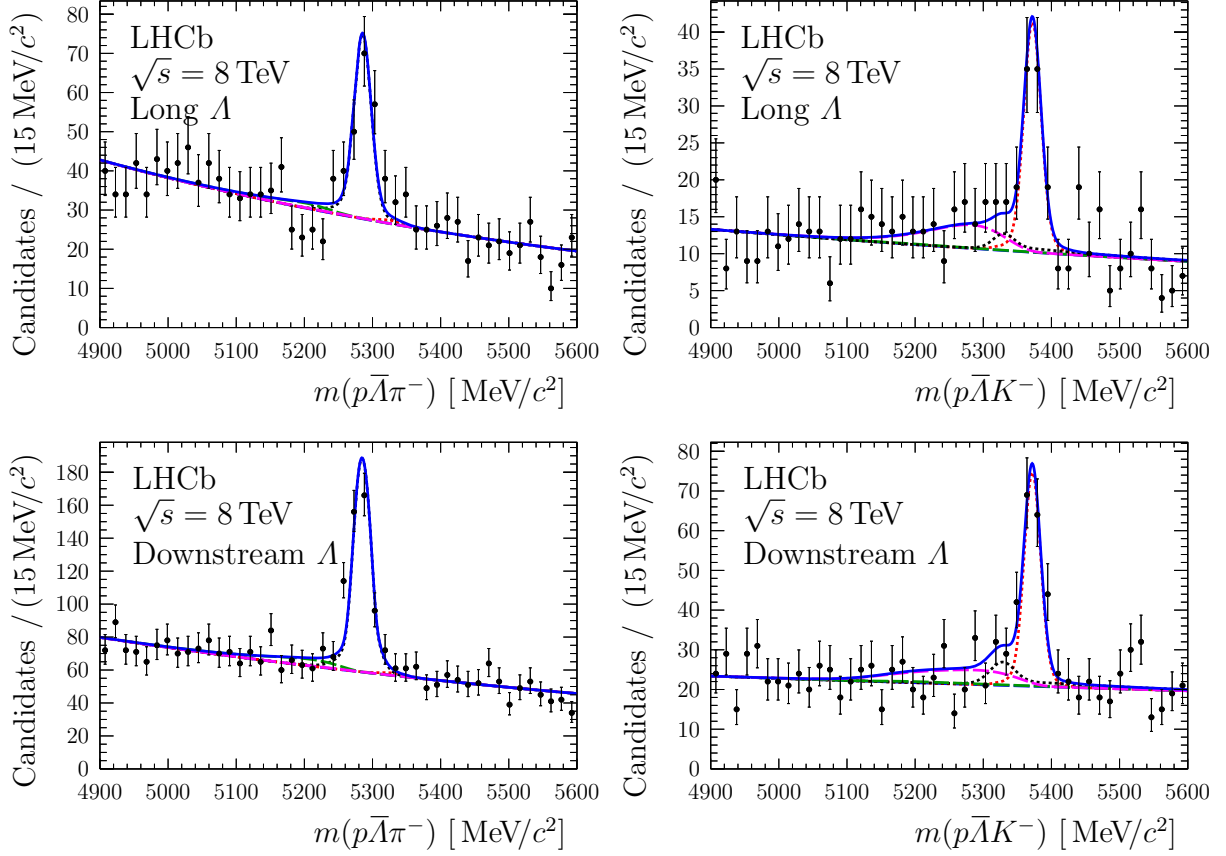


Figure 2: Mass distributions for  $b$ -hadron candidates for (left) the  $p\bar{\Lambda}\pi^-$  and (right) the  $p\bar{\Lambda}K^-$  sample for (top) the long and (bottom) the downstream 2012 categories. The black points represent the data, the solid blue curve the result of the fit, the black (red) dotted curve the  $B^0 \rightarrow p\bar{\Lambda}\pi^-$  ( $B_s^0 \rightarrow p\bar{\Lambda}K^-$ ) contribution, and the green (magenta) dashed curve the contribution from  $B^0 \rightarrow p\bar{\Sigma}^0\pi^-$  ( $B_s^0 \rightarrow p\bar{\Sigma}^0K^-$ ) decays.

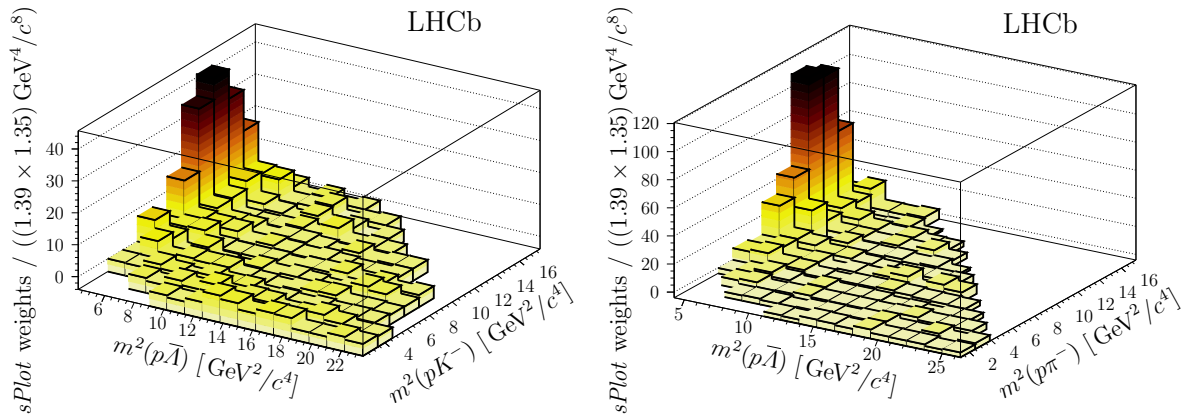


Figure 3: Dalitz plot distribution for (left) the  $B_s^0 \rightarrow p\bar{\Lambda}K^-$  and (right) the  $B^0 \rightarrow p\bar{\Lambda}\pi^-$  decay mode. The bin contents are given by the sum of the  $sPlot$  weights determined from the fits to the  $m(p\bar{\Lambda}h)$  invariant mass for each data sample. The only structure visible is a pronounced enhancement at the  $m(p\bar{\Lambda})$  threshold. The distributions are not corrected for efficiency.

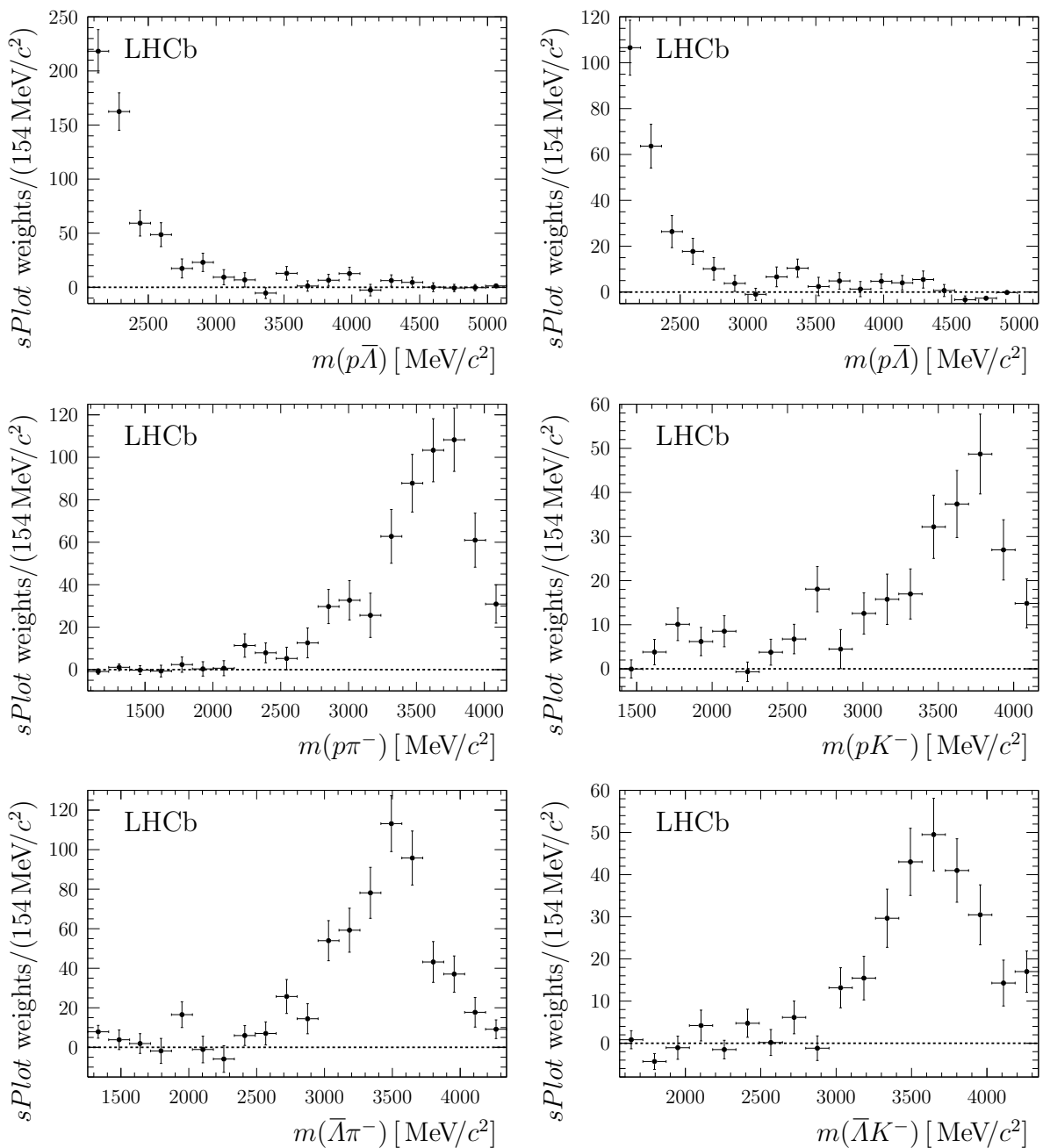


Figure 4: Invariant mass distributions of (top)  $m(p\bar{\Lambda})$ , (middle)  $m(ph^-)$ , and (bottom)  $m(\bar{\Lambda}h^-)$  for (left) the  $B^0 \rightarrow p\bar{\Lambda}\pi^-$  and (right) the  $B_s^0 \rightarrow p\bar{\Lambda}K^-$  signal candidates. The binning is chosen to be sensitive to typical widths of baryon resonances in  $m(ph^-)$  and  $m(\bar{\Lambda}h^-)$ . The background subtraction is performed using the  $sPlot$  technique. The distributions are not corrected for efficiency.

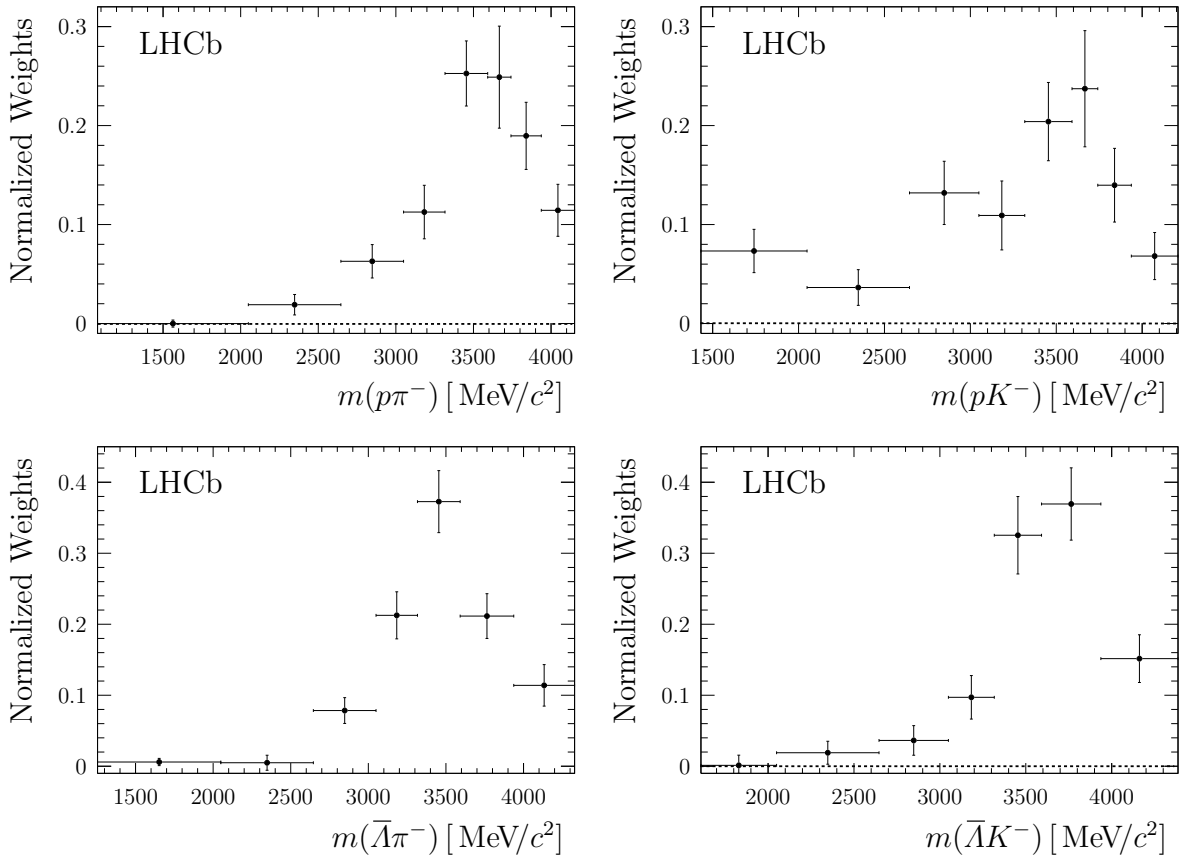


Figure 5: Efficiency-corrected and normalized  $sWeight$  for the invariant mass distributions of (top)  $m(ph^-)$  and (bottom)  $m(\bar{\Lambda}h^-)$  for (left) the  $B^0 \rightarrow p\bar{\Lambda}\pi^-$  and (right) the  $B_s^0 \rightarrow p\bar{\Lambda}K^-$  signal candidates.

Source of uncertainty	Value [%]
Detector acceptance	0.9
Trigger efficiencies	2.2
Tracking efficiencies	0.5
PID uncertainties	1.3
Fit model	9.5
Unknown $B_s^0$ eigenstate composition	3.3
Total of above	10.5
$\mathcal{B} (B^0 \rightarrow p\bar{\Lambda}\pi^-)$	9.2
$f_s/f_d$	5.8

Table 1: Summary of systematic uncertainties relative to the measured  $B_s^0 \rightarrow p\bar{\Lambda}K^-$  branching fraction. The total corresponds to the sum of contributions added in quadrature.